Syngas Production via Ethanol Dry Reforming: Effect of Promoter Type on Al$_2$O$_3$-supported Co Catalysts

Fahim Fayaz[1], Mahadi B. Bahari[1], Huy Nguyen-Phu[2], Chinh Nguyen-Huy[3], Bawadi Abdullah[4] and Dai-Viet N. Vo[1,5,*]

[1]Faculty of Chemical & Natural Resources Engineering, Universiti Malaysia Pahang, Lebuhraya Tun Razak, 26300 Gambang, Kuantan, Pahang, Malaysia

[2]School of Chemical Engineering, University of Ulsan, 93 Daehak-ro, Nam-gu, Ulsan 44610, South Korea

[3]School of Energy & Chemical Engineering, Ulsan National Institute of Science and Technology (UNIST), 50 UNIST-gil, Eonyang-eup, Ulju-gun, Ulsan 689-798, Republic of Korea

[4]Chemical Engineering Department, Universiti Teknologi PETRONAS, Malaysia

[5]Centre of Excellence for Advanced Research in Fluid Flow, Universiti Malaysia Pahang, 26300 Gambang, Kuantan, Pahang, Malaysia

*corresponding author:

e-mail: vietvo@ump.edu.my (D.-V.N. Vo)

Abstract. Lanthanide-promoted (ceria and lanthana) and unpromoted 10%Co/Al$_2$O$_3$ catalysts were synthesized via co-impregnation technique and evaluated for ethanol dry reforming in a quartz fixed-bed reactor at $P_{CO2} = P_{C2H5OH} =$ 20 kPa and reaction temperature of 973 K under atmospheric pressure. Both Co$_3$O$_4$ and CoAl$_2$O$_4$ phases were formed on the surface of promoted and unpromoted catalysts. The reduction of Co$_3$O$_4$ to CoO phase was facilitated by CeO$_2$ or La$_2$O$_3$ addition. C$_2$H$_5$OH conversion improved significantly up to about 1.2 and 1.9 times with the addition of CeO$_2$ and La$_2$O$_3$ promoters, respectively. La-promoted catalyst appeared to be the best catalyst in terms of H$_2$ and CO yields as well as C$_2$H$_5$OH conversion followed by Ce-promoted and unpromoted catalysts.

Keywords: Ethanol dry reforming, Co-based catalysts, Hydrogen, Syngas

1. Introduction

The growing concerns about the depletion of fossil fuels and increasing greenhouse gas emissions have resulted in the urgent exploration of alternative and green energy sources which can contribute to reduce the significant dependence on conventional fuels and utilize efficiently the undesirable greenhouse gasses. Syngas (referring to CO and H$_2$ mixture) has been considered as a potential source for the production of environmentally friendly synthetic fuels. Conventionally, syngas is produced via partial oxidation, steam or dry reforming of methane (Usman *et al.*, 2015). However, methane is also a nonrenewable fossil fuel diminishing in the near future. Thus, there is a requirement for a sustainable and green process for generating syngas. Ethanol dry reforming (EDR) seems to be a promising method for syngas production and receives significant attention from both academic and industrial research since this process not only use a renewable reactant, *viz.*, ethanol to generate

syngas employed as feedstock for downstream methanol production and Fischer-Tropsch synthesis, FTS (Vo and Adesina, 2012) but also mitigate undesirable CO$_2$ greenhouse gas. Additionally, ethanol, which is rich of hydrogen content, readily available, and easily stored, can be simply produced via fermentation of biomass such as lignocellulose, sugar cane or starch-rich materials (Ni *et al.*, 2007; Vicente *et al.*, 2014).

Like other catalytic reforming processes of methane, EDR reaction is commonly carried out using Ni-based catalysts in order to aid the cleavage of C-C and C-O bonds in ethanol (Hu and Lu, 2009; Bellido *et al.*, 2009). However, Ni-based catalysts were easily deactivated during EDR process due to carbon formation through the Boudouard, methane cracking and ethylene polymerization reactions (Zawadzki *et al.*, 2014; Bellido *et al.*, 2009). Lanthanide metals (including La$_2$O$_3$ and CeO$_2$) have been recently employed as dopants or supports for Ni-based catalysts to improve carbon resilience during EDR reaction owing to their strong basic properties, high CO$_2$ adsorption capacity, great oxygen storage capacity and hence excellent coke resistance (Srisiriwat *et al.*, 2009; Mazumder and de Lasa, 2014). In fact, Zawadzki *et al.* (2014) investigated the influence of different types of supports (such as CeO$_2$, Al$_2$O$_3$, ZrO$_2$ and MgO) on Ni-based catalysts for EDR and found that CeO$_2$-supported Ni catalyst exhibited the highest ethanol conversion and catalytic reduction in H$_2$ reducing agent was alleviated. Bahari *et al.* (2017) also reported that 3%La-10%Ni/Al$_2$O$_3$ catalyst appeared to be stable with time-on-stream during EDR reaction due to the redox characteristic of La$_2$O$_3$ promoter.

However, to the best of our knowledge, there are no previous studies about Co-based catalysts with the addition of rare-earth metal oxides for EDR. Thus, the objective of this research is to examine the influence of La and Ce dopants on the physicochemical properties of Co/Al$_2$O$_3$ catalyst and its catalytic performance for EDR reaction.

2. Experimental

2.1. Catalyst preparation

The wetness impregnation and co-impregnation techniques were employed for the synthesis of unpromoted $10\%Co/Al_2O_3$ and $3\%X$-$10\%Co/Al_2O_3$ (X: La or Ce) catalysts, respectively. $Co(NO_3)_2 \cdot 6H_2O$, $La(NO_3)_3 \cdot 6H_2O$ and $Ce(NO_3)_3 \cdot 6H_2O$ (procured from Sigma-Aldrich Chemicals) were used as metal precursors whilst γ-Al_2O_3 support (Puralox SCCa-150/200, Sasol) was previously calcined with flowing air in a Carbolite furnace at temperature of 1023 K for 5 h with a heating rate of 5 K min^{-1}.

An accurately measured amount of these metal precursors was mixed and magnetically stirred with a balanced amount of pretreated γ-Al_2O_3 support for 3 h at ambient temperature. The resulting slurry was subsequently dried in an oven for 24 h at 383 K before it was calcined in air at temperature of 773 K for 5 h with a heating rate of 5 K min^{-1}. Catalysts were also crushed and sieved to the desired particle size of 125-160 μm prior to EDR evaluation.

2.2. Catalyst characterization

The multi-point Brunauer-Emmett-Teller (BET) surface area of γ-Al_2O_3 support, promoted and unpromoted catalysts was measured in a Micromeritics ASAP-2020 apparatus using N_2 adsorption-desorption isotherms at 77 K. Prior to adsorption measurements, all samples were outgassed at 573 K for 1 h in order to remove moisture and volatile compounds. X-ray diffraction (XRD) measurements for both support and catalysts were conducted in a Rigaku Miniflex II system employing Cu target as radiation source (wavelength, $\lambda = 1.5418$ Å). The system was operated at 30 kV and 15 mA whilst all specimens were scanned slowly from 3° to 80° with small scan speed and step size of corresponding 1° min^{-1} and 0.02°.

H_2 temperature-programmed reduction (H_2-TPR) measurements were performed in a Micromeritics AutoChem II-2920 instrument. About 0.1 g of sample was placed in a quartz U-tube and sandwiched by quartz wool. After being pretreated at 373 K for 30 min in flowing He of 50 ml min^{-1} for eliminating volatile materials, specimen was heated to 1173 K with a heating rate of 10 K min^{-1} in 50 ml min^{-1} of $10\%H_2/Ar$ mixture. It was further kept isothermally at this temperature for 30 min in the same gaseous mixture.

2.3. Catalytic activity test

Catalytic tests were performed in a quartz tubular fixed-bed reactor with length, L and outer diameter, $O.D.$ of 17 and 3/8 inches, respectively (see Fig. 1). Syringe pump (KellyMed KL-602 model) was used to accurately feed ethanol into the top of fixed-bed reactor whilst CO_2 gaseous reactant and N_2 diluent gas were precisely regulated by Alicat mass flow controllers. EDR runs were conducted at atmospheric pressure with reaction temperature, T of 973 K and stoichiometric feed composition (with reactant partial pressure, $P_{C2H5OH} = P_{CO2} = 20$ kPa and partial pressure of N_2 diluent gas, P_{N2} of about 61 kPa).

Roughly 0.1 g of catalyst with small average particle size of 125-160 μm was mounted by quartz wool in the middle of quartz tube reactor. Prior to each EDR reaction, H_2 reduction was conducted using 60 ml min^{-1} of $50\%H_2/N_2$ with heating rate of 10 K min^{-1} from ambient temperature to 923 K. Sample was further kept isothermally at this reduction temperature for 2 h before heating up to EDR reaction temperature of 973 K in flowing N_2 (60 ml min^{-1}) inert gas. High gas hourly space velocity (GHSV) of 42 L g_{cat}^{-1} h^{-1} was also employed for all runs to ensure the negligible presence of internal and external transport intrusions. The composition of gaseous effluent from the outlet of fixed-bed reactor was analyzed in an Agilent 6890 GC Gas Chromatograph Series installed with a thermal conductivity detector (TCD).
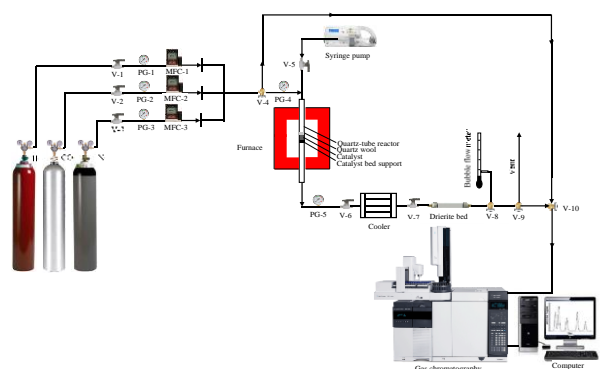

Figure 1. Schematic of experimental set-up for EDR

3. Results and discussion

3.1. BET surface area measurements

Calcined γ-Al_2O_3 support possessed BET surface area of 175.3 m^2 g^{-1}. However, a lower BET surface area observed for $10\%Co/Al_2O_3$ catalyst (143.1 m^2 g^{-1}) was unavoidable due to pore blockage associated with Co diffusion into Al_2O_3 support. Interestingly, both $3\%Ce$-$10\%Co/Al_2O_3$ and $3\%La$-$10\%Co/Al_2O_3$ catalysts had BET surface area of corresponding 142.2 and 136.0 m^2 g^{-1} comparable to that of unpromoted $10\%Co/Al_2O_3$ catalyst. This observation would suggest that La and Ce promoters were well dispersed on catalyst surface.

3.2. X-ray diffraction analysis

The XRD patterns of γ-Al_2O_3 support, promoted and unpromoted $10\%Co/Al_2O_3$ catalysts are shown in Fig. 2. The crystalline phases of samples were identified based on the Joint Committee on Powder Diffraction Standards (JCPDS) database (JCPDS powder diffraction file, 2000). The X-ray diffractogram of γ-Al_2O_3 support was also used as a reference for comparing with promoted and unpromoted catalysts. As seen in Fig. 2, the typical peaks of γ-Al_2O_3 phase (at 2θ of 18.92°, 32.88°, 37.10°, 45.61°

and 67.17°) were detected on support and all catalysts (JCPDS card No. 04-0858). Additionally, the diffraction peaks located at 2θ = 31.45°, 37.10°, 44.79° and 55.66° were assigned to Co_3O_4 phase (JCPDS card No. 74-2120) while the spinel $CoAl_2O_4$ phase observed at 2θ range of 59.51° and 65.38° (JCPDS card No. 82-2246) on the surface of promoted and unpromoted catalysts would suggest the strong interaction between γ-Al_2O_3 support and CoO phase (see Fig. 2(b)-(d)).

As seen in Fig. 2(c), CeO_2 phase was also detected at 2θ of 28.57° on Ce-promoted catalyst (Abd El-Hafiz *et al.*, 2015). It could be probably formed from $Ce(NO_3)_3$ decomposition to Ce_2O_3 phase followed by oxidation to CeO_2 phase during air-calcination. However, the characteristic diffraction peaks for La_2O_3 phase at 2θ of 29.87° and 53.42° (Bahari *et al.*, 2017) were not detected on the surface of La-promoted catalyst (see Fig. 2(d)), probably due to its high metal dispersion and hence smaller La_2O_3 crystallite size than the detection limit of XRD measurement.
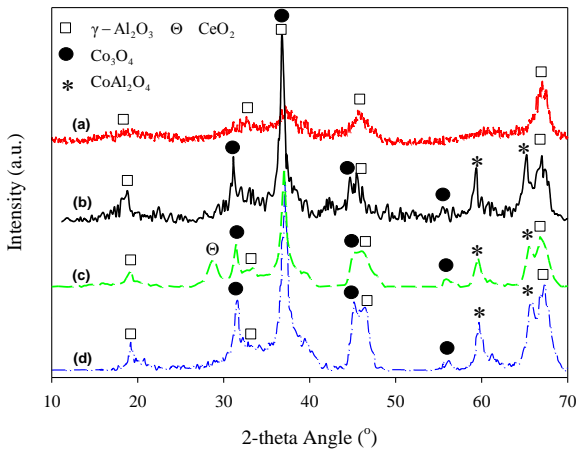

Figure 2. XRD patterns of (a) calcined γ-Al_2O_3 support, (b) 10%Co/Al_2O_3, (c) 3%Ce-10%Co/Al_2O_3 and (d) 3%La-10%Co/Al_2O_3 catalysts

3.3. H₂ temperature-programmed reduction

H_2 reduction profiles of both catalyst and γ-Al_2O_3 support are shown in Fig. 3. There was no peak detected on γ-Al_2O_3 support (see Fig. 3(a)) whilst three discrete peaks (P1, P2 and P3) were observed for promoted and unpromoted catalysts (see Fig. 3(b)-(d)). The resistance of γ-Al_2O_3 support to H_2 reduction would indicate that the detected peaks (P1, P2 and P3) belonged to the reduction of active metal oxides. In fact, the first peak P1 ranging from 570 to 707 K was attributed to the reduction of Co_3O_4 to CoO phase (Papageridis *et al.*, 2016) whilst the second peak (P2 of about 708-850 K) was assigned to CoO reduction to metallic Co^0 form (Jabbour *et al.*, 2014). In addition, the small shoulder at high reduction temperature (P3 of 851-1000 K) was ascribed to the reduction of $CoAl_2O_4$ phase which possesses strong metal-support interaction and hence great resistance to H_2 reduction (Hull and Trawczynski, 2014). As seen in Fig. 3(b)-(d), the reduction temperature for Co_3O_4 to CoO phase (peak P1)

was lower with promoter addition probably due to the high electron density donated by CeO_2 or La_2O_3 phase (Fayaz *et al.*, 2016; Zhi *et al.*, 2011).
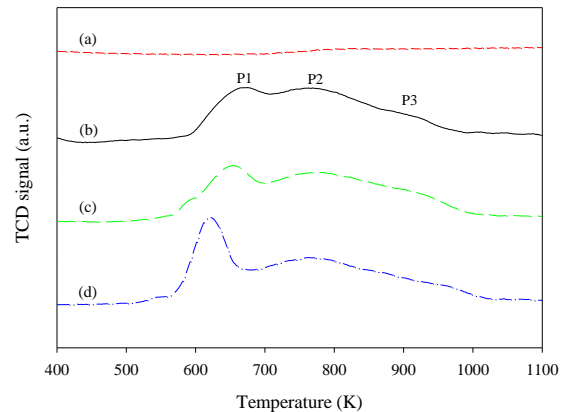

Figure 3. H_2-TPR profiles of (a) calcined γ-Al_2O_3 support, (b) 10%Co/Al_2O_3, (c) 3%Ce-10%Co/Al_2O_3 and (d) 3%La-10%Co/Al_2O_3 catalysts

3.4. Ethanol dry reforming evaluation

Fig. 4 shows the influence of promoter addition on C_2H_5OH conversion with time-on-stream (TOS) of 10%Co/Al_2O_3 catalyst at $P_{CO2} = P_{C2H5OH}$ = 20 kPa and reaction temperature of 973 K. C_2H_5OH conversion of both promoted and unpromoted 10%Co/Al_2O_3 catalysts initially dropped with time-on-stream (TOS) and reached to steady state at beyond 5 h on-stream. As seen in Fig. 4, C_2H_5OH conversion improved with the addition of dopants in the order; 3%La-10%Co/Al_2O_3 > 3%Ce-10%Co/Al_2O_3 > 10%Co/Al_2O_3 catalyst. In fact, La and Ce additions enhanced C_2H_5OH conversion of 10%Co/Al_2O_3 catalyst up to 1.9 and 1.2 times, respectively. Interestingly, both H_2 and CO yields also increased with promoter addition in the same order; La-promoted > Ce-promoted > unpromoted catalysts during 8 h on-stream (see Fig. 5). The enhancement in reactant conversion and product yield with La_2O_3 and CeO_2 dopants was reasonably owing to the basic property of dopants (Foo *et al.*, 2011) facilitating the adsorption of CO_2 reactant on catalyst surface and high oxygen storage capacity of these promoters hindering carbon deposition (Li *et al.*, 2015).
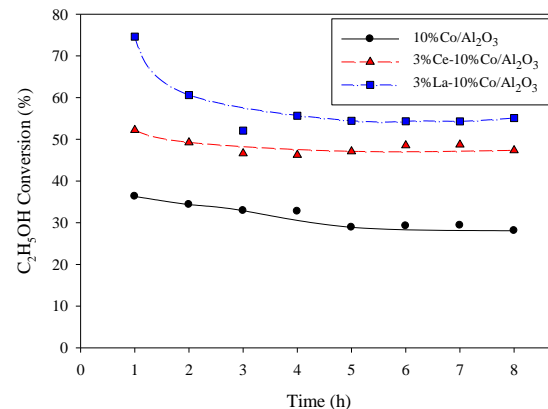
Figure 4. Effect of promoter addition on C_2H_5OH conversion with time-on-stream over Al_2O_3-supported Co catalysts at $P_{CO2} = P_{C2H5OH} = 20$ kPa and $T = 973$ K
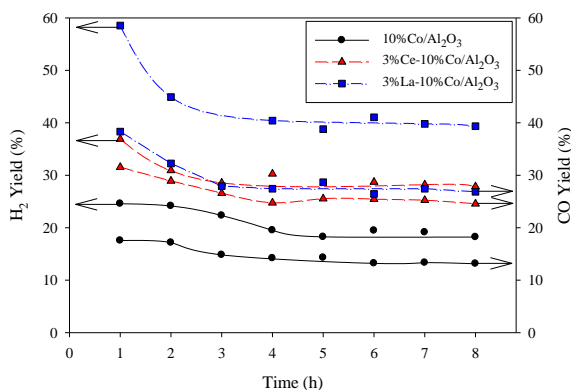

Figure 5. Effect of promoter addition on H_2 and CO yields with time-on-stream over Al_2O_3-supported Co catalysts at $P_{CO2} = P_{C2H5OH} = 20$ kPa and $T = 973$ K

4. Conclusions

Both promoted and unpromoted $10\%Co/Al_2O_3$ catalysts were synthesized using a co-impregnation method and evaluated for EDR reaction at stoichiometric feed ratio. XRD measurement indicated the presence of both Co_3O_4 and $CoAl_2O_4$ phases on the surface of promoted and unpromoted catalysts. The doping of La_2O_3 and CeO_2 enhanced electron density on the surface of catalyst and hence easing the reduction of Co_3O_4 to CoO phase during H_2-TPR. Catalytic stability was stable within 5-8 h on-stream for both promoted and unpromoted catalysts. La-promoted catalyst appeared to be the optimal catalyst followed by Ce-promoted and unpromoted catalysts in terms of C_2H_5OH conversion and product (i.e., H_2 and CO) yield probably due to the basic property and high oxygen storage capacity of dopants.

References

Abd El-Hafiz D.R., Ebiad M.A., Elsalamony R.A., and Mohamed L.S. (2015), Highly stable nano Ce–La catalyst for hydrogen production from bio-ethanol, *RSC Advances*, **5**, 4292–4303.

Bahari M.B., Phuc N.H.H., Alenazey F., Vu K.B., Ainirazali N. and Vo D.-V.N. (2017), Catalytic performance of La-Ni/Al$_2$O$_3$ catalyst for CO$_2$ reforming of ethanol, *Catalysis Today*, DOI: 10.1016/j.cattod.2017.02.019.

Bellido J.D.A., Tanabe E.Y. and Assaf E.M. (2009), Carbon dioxide reforming of ethanol over Ni/Y$_2$O$_3$–ZrO$_2$ catalysts, *Applied Catalysis B: Environmental*, **90**, 485–488.

Fayaz F., Danh H.T., Nguyen-Huy C., Vu K.B., Abdullah B. and Vo D.-V.N. (2016), Promotional Effect of Ce-dopant on Al$_2$O$_3$-supported Co Catalysts for Syngas Production via CO$_2$ Reforming of Ethanol, *Procedia Engineering*, **148**, 646-653.

Foo S.Y., Cheng C.K., Nguyen T.H. and Adesina A.A. (2011), Evaluation of lanthanide-group promoters on Co-Ni/Al$_2$O$_3$ catalysts for CH$_4$ dry reforming, *Journal of Molecular Catalysis A: Chemical,* **344**, 28–36.

Jabbour K., Hassan N.E., Casale S., Estephane J. and Zakhem H.E. (2014), Promotional effect of Ru on the activity and stability of Co/SBA-15 catalysts in dry reforming of methane, *International Journal of Hydrogen Energy*, **39,** 7780–7787.

JCPDS Powder Diffraction File (2000), International Centre for Diffraction Data. Swarthmore, PA.

Hu X. and Lu G. (2009), Syngas production by CO$_2$ reforming of ethanol over Ni/Al$_2$O$_3$ catalyst, *Catalysis Communications*, **10**, 1633–1637.

Hull S. and Trawczynski J. (2014), Steam reforming of ethanol on zinc containing catalysts with spinel structure, *International Journal of Hydrogen Energy*, **39**, 4259–4265.

Li D., Zeng L., Li X., Wang X., Ma H., Assabumrungrat S. and Gong J. (2015), Ceria-promoted Ni/SBA-15 catalysts for ethanol steam reforming with enhanced activity and resistance to deactivation, *Applied Catalysis B: Environmental,* **176–177**, 532–541.

Mazumder J. and de Lasa H.I. (2014), Ni catalysts for steam gasification of biomass: Effect of La$_2$O$_3$ loading, *Catalysis Today*, **237**, 100–110.

Ni M., Leung D.Y.C. and Leung M.K.H. (2007), A review on reforming bio-ethanol for hydrogen production, *International Journal of Hydrogen Energy*, **32**, 3238–3247.

Papageridis K.N., Siakavelas G., Charisiou N.D., Avraam D.G., Tzounis L., Kousi K. and Goula M.A. (2016), Comparative study of Ni, Co, Cu supported on γ-alumina catalysts for hydrogen production via the glycerol steam reforming reaction, *Fuel Processing Technology*, **152**, 156–175.

Srisiriwat N., Therdthianwong S. and Therdthianwong A. (2009), Oxidative steam reforming of ethanol over Ni/Al$_2$O$_3$ catalysts promoted by CeO$_2$, ZrO$_2$ and CeO$_2$-ZrO$_2$, *International Journal of Hydrogen Energy*, **34**, 2224–2234.

Usman M., Daud W.M.A.W., and Abbas H.F. (2015), Dry reforming of methane: Influence of process parameters – A review, *Renewable and Sustainable Energy Reviews*, **45**, 710-744.

Vicente J., Montero C., Ereña J., Azkoiti M.J., Bilbao J. and Gayubo A.G. (2014), Coke deactivation of Ni and Co catalysts in ethanol steam reforming at mild temperatures in a fluidized bed reactor, *International Journal of Hydrogen Energy*, **39**, 12586–12596.

Vo D.-V.N. and Adesina A.A. (2012), A potassium-promoted Mo carbide catalyst system for hydrocarbon synthesis, *Catalysis Science & Technology*, **2**, 2066-2076.

Zawadzki A., Bellido J.D.A., Lucrédio A.F. and Assaf E.M. (2014), Dry reforming of ethanol over supported Ni catalysts prepared by impregnation with methanolic solution, *Fuel Processing Technology*, **128**, 432–440.

Zhi G., Guo X., Wang Y., Jin G., Guo X. (2011), Effect of La$_2$O$_3$ modification on the catalytic performance of Ni/SiC for methanation of carbon dioxide, *Catalysis Communications*, **16**, 56–59.